Wavelet Denoising by Using Linear-Phase NPR-QMF Banks

Mitko Kostov and Cvetko Mitrovski

***Abstract* – In this paper we compare the near-perfect reconstruction (NPR) quadrature mirror filter (QMF) design, versus perfect reconstruction (PR)-QMF design in terms of the flexibility of the design and the design filter characteristics, and their efficiency for denoising of the signals based on wavelet shrinkage technique.**

***Keywords* – Near perfect reconstruction, QMF bank, signal-dependent noise, threshold, wavelet domain denoising.**

I. INTRODUCTION

There are many methods, both in space and in a transform domain, for noise removal from the images [1-12]. In cases when the transformation of the original noisy image is adequately chosen, the energy of the signal will be concentrated into a small number of coefficients. One possible choice is to process signals in the discrete wavelet transform (DWT) domain, while other choice is the Fourier transform of a signal which contains energy at all frequencies. Until now, the methods based on wavelet domain filtering use filter banks that satisfy perfect reconstruction (PR) condition.

In this paper we want to show that for denoising purposes a signal can be successfully decomposed and reconstructed by using linear phase near-perfect reconstruction (NPR) QMF banks as an alternative to the well known wavelet filter banks. Even more, using NPR-QMF banks can yield with competitive or even better results. Wavelet shrinkage involves discarding some of the wavelet coefficients and even though wavelet filters satisfy perfect reconstruction condition, the reconstructed signal differs from the original one. Moreover, the transfer characteristic of some of the known wavelets does not have strictly linear phase. However, a linear phase NPR-QMF bank introduces a reconstruction error which is a design parameter in the process of designing the filter bank and hence it can be chosen relatively small. So, if the error introduced by the NPR bank is smaller than the error obtained when known (PR) wavelets are used, the NPR filters can be considered as good filters for denoising purposes.

The paper is organized as follows. The NPR-QMF banks design and wavelet theory are briefly outlined in Sections II and III, respectively. In Section IV we discuss advantages and drawbacks of NPR-QMF filters and commonly used filters. In Section V we compare the filters performances by denoising 1-D and 2-D deterministic signals contaminated with signal-dependent noise. At the end, Section VI concludes the paper.

Mitko Kostov and Cvetko Mitrovski are with the Faculty of Technical Sciences, I.L.Ribar bb, 7000 Bitola, Macedonia, E-mails: mitko.kostov@uklo.edu.mk, cvetko.mitrovski@uklo.edu.mk

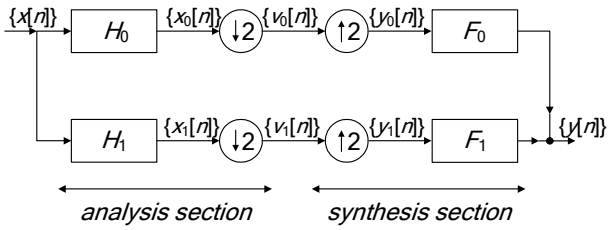

Fig.1. Two-channel filter bank.

II. DESIGN OF TWO-CHANNEL QMF BANKS

The basic block of a two-channel QMF bank consists four even length N linear phase FIR filters, H_0, H_1, F_0, F_1, with impulse responses $h_0[n]$, $h_1[n]$, $f_0[n]$, $f_1[n]$, respectively, out of which H_0, $H_1$are low pass while F_0, F_1 are high pass filters as shown in Fig. 1.

The most commonly used filters for this realization of the filter bank, are the quadrature mirror filters H_0, H_1, F_0, F_1 which satisfy the following property:

$$H_1(e^{j\omega}) = H_0(e^{j(\omega-\pi)}),$$

$$F_0(e^{j\omega}) = H_0(e^{j\omega}),\ F_1(e^{j\omega}) = H_1(e^{j\omega}). \qquad (1)$$

Due to this property, the design problem is simplified, since the coefficients of all the filters are obtained from the lowpass prototype filter coefficients.

In case of PR, the filter coefficients are determined by minimization of the error function between the output and the input of the bank, $e(n) = u_{in}(n) - u_{out}(n)$, in the least-square sense. In our work we propose design of NPR-QMF filter, obtained by minimization of the following error function

$$E = E_r + \alpha E_s, \qquad (2)$$

subject to the filter length, N, and their cut–of frequency ω_s, where: $E_r = \int_0^{\pi} W(\omega)[e_r(\omega)]^2 d\omega$, $E_s = \int_{\omega_s}^{\pi} \left|H_0(e^{j\omega})\right|^2 d\omega$, $e_r(\omega) = \left|H_0(e^{j\omega})\right|^2 + \left|H_0(e^{j(\omega+\pi)})\right|^2 - 1$, $W(\omega)$ is a properly chosen weighting function and α is the relative weight between the measure of the total error signal energy, E_r, and the measure of the error signal energy in the stop band, E_s.

TABLE I
PROTOTYPE FILTER COEFFICIENTS FROM A NPR-QMF BANK

$h_0[0-5]$ =	–0.0095	0.0403	–0.0126	–0.1303
$h_0[11-6]$	0.1407	0.6786		

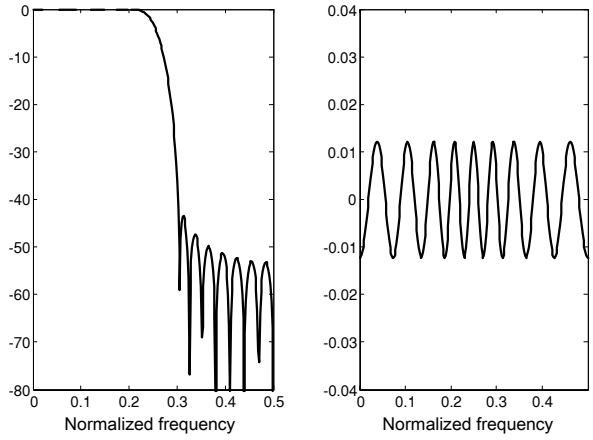

Fig 2. The magnitude responses of the prototype filter and the overall reconstruction error.

III. DISCRETE WAVELET TRANSFORM

In series expansion of discrete-time function f,

$$f(t) = \sum_{j=1}^{J} \sum_{k=1}^{2^{-j}M} d_{jk}\psi_{jk}(t) + \sum_{k=1}^{2^{-J}M} c_{Jk}\phi_{Jk}(t), \qquad (3)$$

ψ_{jk} and ϕ_{jk} denote wavelet and scaling functions

$$\psi_{jk}(t) = 2^{-k/2}\psi(2^{-k}t - n), \qquad (4)$$

a_{Jk} and d_{jk} are approximation and detail coefficients, and j and k are dilatation and translation indexes, respectively. The mother and scaling functions are defined by:

$$\psi(t) = \sum_n 2^{1/2} h_1 \psi(2t - n) \qquad (5)$$

$$\phi(t) = \sum_n 2^{1/2} h_0 \phi(2t - n) \qquad (6)$$

The estimation of d_{jk} and c_{Jk} is carried out through an iterative decomposition algorithm, which uses two QMF filters, h_0 and h_1.

IV. NPR-QMF DESIGN

The idea and motivation for using a NPR-QMF bank as a replacement of a PR-QMF bank in combination with the wavelet shrinkage denoising technique is based on the fact that in both cases the inherent nonlinearities of the wavelet filtrating technique causes reconstruction error of the input signal.

In this section we are presenting characteristics of the NPR-QMF filter designed by using the proposed algorithm in section II, with the design parameters: filter length, $N = 12$ and its stop band cut off frequency, $f_s = 0.6\pi$.

The coefficients of designed low pass filter, h_0, are given in Table I, while its frequency response is given in Fig. 2a. This filter has linear phase, good pass-band and transition band characteristics, but it produces certain overall reconstruction error, given in Fig. 2b.

TABLE II
COMPARISON OF THE SLOPES OF THE TRANSITION BANDS OF THE MOST FREQUENTLY USED FILTERS WITH NPR-QMF FILTERS

	$\omega_p(\times\pi)$ (1)	$\omega_s(\times\pi)$ (2)	$a(\omega_p)$ (3)	$a(\omega_s)$ (4)	slope (dB/rad/s) (5=(4–3)/(2–1))
NPR QMF (N=32)	0.50	0.60	–2.99	–33.23	**–98.54**
NPR QMF (N=12)	0.49	0.66	–2.93	–33.70	–58.99
Db3	0.50	0.88	–2.96	–34.89	–26.28
Db6	0.50	0.79	–3.01	–34.89	–34.54
sym5	0.50	0.82	–2.95	–34.81	–31.86
sym6	0.50	0.79	–3.01	–34.80	–34.54
coif4	0.50	0.75	–3.01	–34.57	–39.87
coif5	0.50	0.73	–3.01	–34.95	–44.49

V. EXPERIMENTAL RESULTS

In this section, we compare the efficiency of the NPR-QMF filter design versus PR-wavelet filter design, on basis of their frequency characteristics, and the efficiency of the both designs in signal denoising by wavelet shrinkage technique.

The NPR-QMF filters are with filter lengths: $N = 12$ and $N = 32$ and stop band cut-off frequency equal to 0.6π

The results of the comparison among the NPR-QMF filters and the PR wavelet filters are expressed in Table II, in terms of their transition band slopes calculated as a slope of their frequency responses among the cut-off frequency and the frequency for which the amplitude response is 35 dB lower than in the pass-band. The advantage of the NPR-QMF is obvious. Further more, NPR-QMF filters have better pass band and stop band characteristics versus biorthogonal 9/7 and Daubechies wavelet filters in terms of their magnitude responses as illustrated in Fig. 3 and Fig. 4. From those figures and from Table II, it is obvious that NPR-QMF filters have better magnitude responses than both the Daubechies and Simlet's family wavelet filters and they do have linear phase while the wavelet filters do not have.

Comparing NPR-QMF filters and the filter that corresponds to the Meyer wavelet, the second is only approximation of FIR filter. Fig. 4b shows its impulse response.

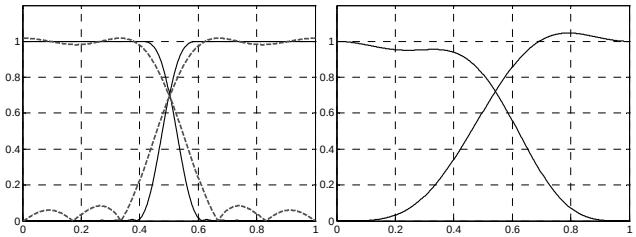

Fig 3. Comparison of magnitude responses of NPR-QMF and biorthogonal filters: (a) NPR-QMF with $\omega_s = 0.6\pi$ and filter lengths $N = 12$ and 32; (b) biorthogonal 9/7 filters.

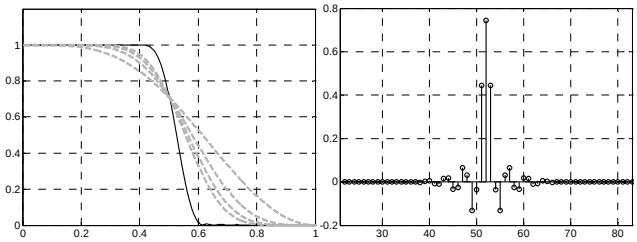

Fig. 4. (a) Magnitude responses of NPR-QMF bank filters ($N = 32$, $\omega_s = 0.6\pi$) (black full line) versus responses of filters that correspond to Daubechies family (db2, db4, db6, db8) (grey lines); b) impulse response of the corresponding filter to the Meyer wavelet.

The frequency responses of the filters that correspond to wavelets from Daubechies and Simlets families, have more zeros at π and the wavelet functions have more vanishing moments (the number is equal to the half of the filter length). Hence, by using such wavelet functions, the signal power is concentrated in small number of wavelet coefficients, which should be kept non-modified by the shrinkage procedure. This stands if the signal is smooth. More zeros at π means that smother signals are better approximated.

In order quantitatively to compare the denoising capabilities of the designed filters we use 1D and 2D test signals shown in Fig. 5-left. The 1D test signal was obtained by adding a Poisson noise to the corresponding artificially generated signal (right), while the 2D test signals (right), were generated from the corresponding phantom images (left) by summing a bell shaped random 2D signals with Gaussian distribution around each pixel, with total intensity proportional to the pixel intensity on the original phantom image. Since the obtained test images have significantly less energy then the original phantom images, we normalized them before the denoising test.

All test signals are denoised by using both: the NPR-QMF bank filter (Table I) and different types of PR wavelets, and the results were compared with the original signals in the average mean square error (MSE) sense.

From the results shown in Figs. 6-9, it is obvious that NPR-QMF banks are concurrent to the PR wavelet filters both for 1D and 2D signal denoising by using wavelet shrinkage technique.

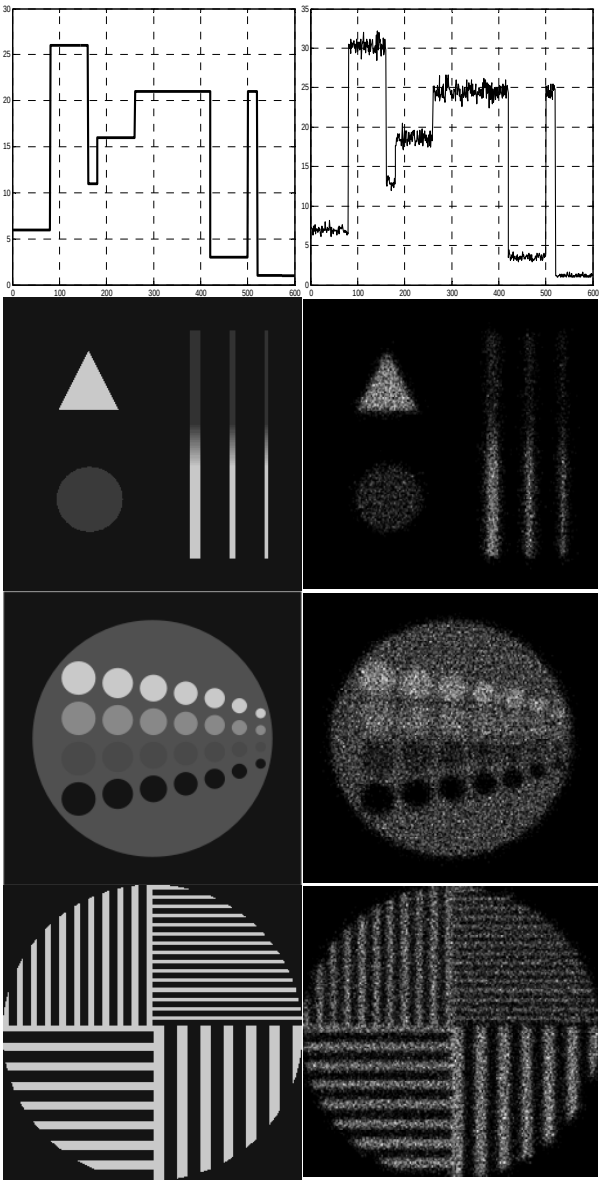

Fig. 5. Deterministic signals and their noisy versions: 1D signal, Phantom, Circles, Bars.

VI. CONCLUSION

In this paper we compare the efficiency of the NPR-QMF filter design versus PR-wavelet filters on basis of test signal denoising. The results show that NPR-QMF banks, designed by choosing low values for α ($\alpha<10^{-2}$), are competitive to the PR wavelets, in terms of design flexibilities and their efficiency on denoising both 1D and 2D signals, by using wavelet shrinkage technique.

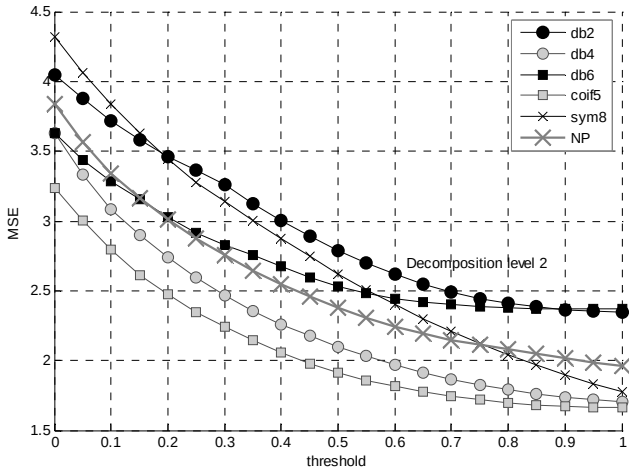

Fig. 6. Comparison of different wavelet filters for the 1D signal and different threshold values.

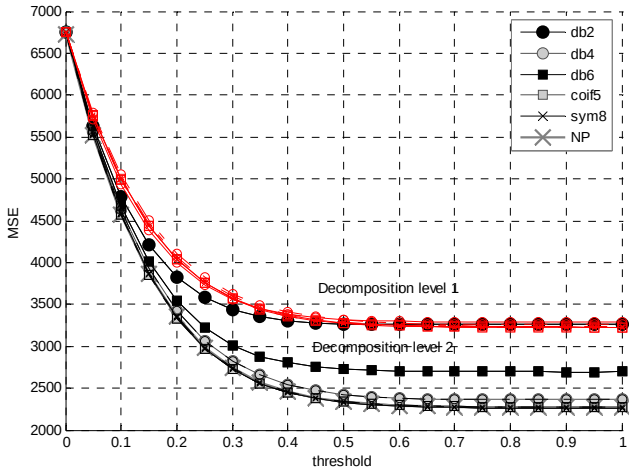

Fig. 7. Comparison of different wavelet filters for the image Bars and different threshold values.

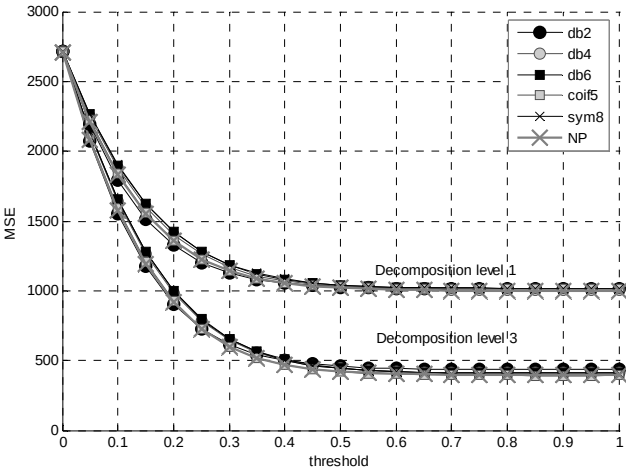

Fig. 8. Comparison of different wavelet filters for the image Circles and different threshold values.

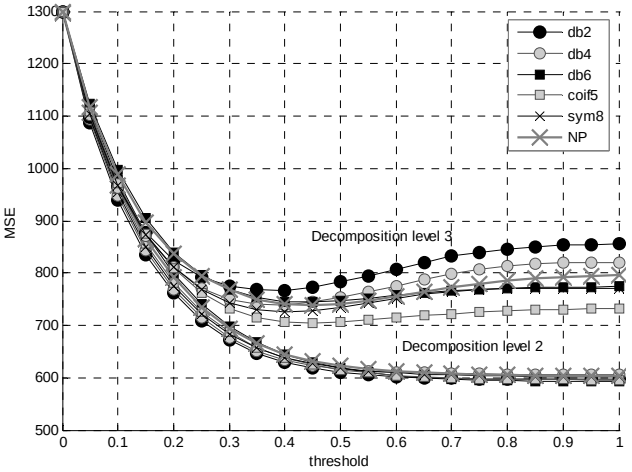

Fig. 9. Comparison of different wavelet filters for the image Phantom and different threshold values.

REFERENCES

[1] D. L. Donoho and I. M. Johnstone, "Ideal Spatial Adaptation via Wavelet Thresholding", *Biometrika*, vol. 81, pp. 425-455, 1994;

[2] Y. Xu, J. B. Weaver, D. M. Healy, Jr., and J. Lu "Wavelet Transform Domain Filters: A Spatially Selective Noise Filtration Technique", *IEEE Trans. on Image Processing*, vol. 3, no. 6, pp. 747-758, Nov. 1994;

[3] Robert D. Nowak, Richard G. Baraniuk, "Wavelet-Domain Filtering for Photon Imaging Systems", *IEEE Trans. Image Processing*, vol. 8, Iss. 5, p. 666-678, May 1999;

[4] S. Zhong, V. Cherkassky, "Image Denoising using Wavelet Thresholding and Statistical Learning Theory", *IEEE Trans. on Image Processing*, Feb. 1999.

[5] S.G. Chang, B. Yu, M. Vetterli, "Adaptive Wavelet Thresholding for Image Denoising and Compression", *IEEE Trans. Image Processing*, vol. 9, pp. 1532-1546, Sept. 2000;

[6] S. Zhong, V. Cherkassky, "Image Denoising using Wavelet Thresholding and Model Selection", *Proceedings of Int. Conf. on Image Processing*, vol. 3, pp. 262-265, Vancouver, BC, Canada, Sept. 2000.

[7] L. Sendur, I.W. Selesnick, "Bivariate shrinkage with local variance estimation", *IEEE Signal Process. Letters*, vol. 9, no. 12, pp. 438–441, Dec. 2002;

[8] P. Bao and L. Zhang "Noise Reduction for Magnetic Resonance Images via Adaptive Multiscale Products Thresholding", *IEEE Trans. on Medical Processing*, vol. 22, no. 9, pp. 1089-1099, Sept. 2003;

[9] J. Ge, G. Mirchandani "Softening the Multiscale Product Method for Adaptive Noise Reduction", *Thirty-Seventh Asilomar Conf. on Signals, Systems and Computers*, vol.2, pp. 2124-2128, 9-12 Nov. 2003;

[10] E. J. Balster, Y. F. Zheng and R. L. Ewing "Feature-Based Wavelet Shrinkage Algorithm for Image Denoising", *IEEE Trans. on Image Processing*, vol. 14, no. 12, pp. 2024-2039, Dec. 2005;

[11] A. Pižurica, W. Philips, "Estimating the probability of the presence of a signal of interest in multiresolution single- and multiband image denoising", *IEEE Trans. Image Process.*, vol. 15, no. 3, pp. 645–665, Mar. 2006;

[12] F. Luisier, T. Blu, M. Unser, "A New SURE Approach to Image Denoising: Interscale Orthonormal Wavelet Thresholding", *IEEE Trans. on Image Proc.* vol. 16, pp. 593-606, Mar. 2007.